

## Untwinned single crystals of $\text{YBa}_2\text{Cu}_3\text{O}_{7-\delta}$ : An optical investigation of the $a$ - $b$ anisotropy

C. Thomsen, M. Cardona, B. Gegenheimer, R. Liu, and A. Simon

*Max-Planck-Institut für Festkörperforschung, Heisenbergstrasse 1, D-7000 Stuttgart 80, Federal Republic of Germany*

(Received 24 February 1988)

We report the preparation and investigation of untwinned single-crystal specimens of  $\text{YBa}_2\text{Cu}_3\text{O}_{7-\delta}$ . They were grown from a flux without oxygen annealing treatment, show a  $T_c$  of 89 K, a transition width of  $\Delta T_c \approx 3$  K, and an almost complete magnetic shielding effect. The Raman scattering reflects the orthorhombic symmetry and untwinned structure of the crystals. Furthermore, we found in this crystal that the softening of the Raman mode at  $335 \text{ cm}^{-1}$  through  $T_c$  occurs within a temperature region 10 times narrower than previously reported.

Many reports on the lattice vibrations of the new class of superconductors have appeared. Preliminary mode assignments based on investigations of ceramic materials<sup>1-5</sup> became precise when the symmetries of the Raman-active modes were determined by measurements on single crystals.<sup>6-9</sup> The Raman tensor elements have been obtained for the Raman-active modes at 120, 154, 335, 435, and  $500 \text{ cm}^{-1}$ .<sup>6</sup> They reflect tetragonal symmetry; however, all measurements on crystals reported so far, to our knowledge, were made on species twinned in the  $a$ - $b$  direction. They could hence yield no information about possible orthorhombic symmetry features. In this Rapid Communication we report that the modes mentioned above have, in fact, orthorhombic symmetry in an essentially single-domain crystal. The Raman spectra change when  $a$  and  $b$  axes are interchanged with respect to the orientation of the light polarization vectors. In addition, we observe two defect-induced ir-active (Raman-forbidden) modes which should show appreciable polarizability only in the directions of the chains of the superconductors ( $b$  axis) and thus reflect a strong symmetry breaking. The Raman spectra, hence, witness the underlying orthorhombicity of the superconductor.

In particular we studied the softening of the Raman-active phonon at  $335 \text{ cm}^{-1}$  when cooling below  $T_c$ . This softening implies the existence of a gap above  $335 \text{ cm}^{-1}$  and links this phonon to the superconductivity mechanism. Previous publications report a gradual shift to lower frequencies roughly when the sample is cooled below  $T_c$ .<sup>10,11</sup> We find, however, that in the untwinned single crystal, the shift occurs within a much narrower temperature interval.

The single crystals were grown from a partially melting mixture of 66.67 mol%  $\text{CuO}$ , 26.67 mol%  $\text{BaCO}_3$ , and 6.66 mol%  $\text{YO}_{1.5}$  by a slow-cooling method.<sup>12</sup> The starting material was heated in air to a maximum temperature of  $1050^\circ\text{C}$ , held there for 3 h, and then cooled slowly at  $1.7^\circ\text{C/h}$  from  $1050^\circ\text{C}$  to  $850^\circ\text{C}$  and at  $10^\circ\text{C/h}$  from  $850^\circ\text{C}$  to room temperature. Impurities from crucible materials generally have a deteriorating effect on the structure and superconducting properties of  $\text{YBa}_2\text{Cu}_3\text{O}_7$ .<sup>12,13</sup> We found that a (Zn, Ti)-doped  $\text{SnO}_2$  crucible produced the best results for crystal growth. No Sn incor-

poration in the crystals was detected by energy dispersive x-ray analysis (EDAX). Without further annealing in oxygen, the crystals showed a sharp superconducting transition at  $T_c = 89$  K. As-grown crystals had *orthorhombic* symmetry: x-ray precession photographs showed that most of the crystals were twinned according to the (110) twin law.<sup>14,15</sup> Several of them, however, were found with untwinned domains up to about  $40 \mu\text{m}$  in size (Fig. 1).

The crystal used for the Raman measurements consisted of two single domains of identical orientation separated by a narrow twinned region (approximately 10%). The twinned region is easily recognized microscopically by a pattern of narrow stripes parallel to [110]. Precession photographs of this crystal showed orthorhombic metric with  $a = 381$  and  $b = 388$  pm.

In Fig. 2, we show Raman backscattering spectra of

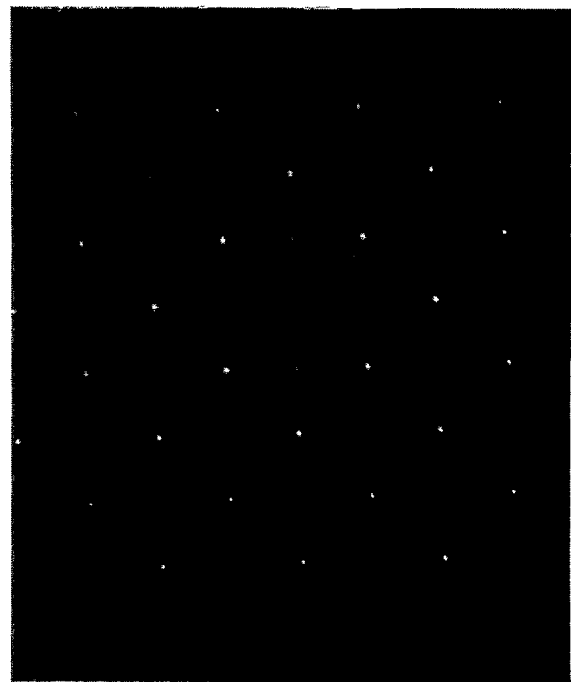


FIG. 1. X-ray precession photograph of an untwinned single crystal of  $\text{YBa}_2\text{Cu}_3\text{O}_{7-\delta}$ .

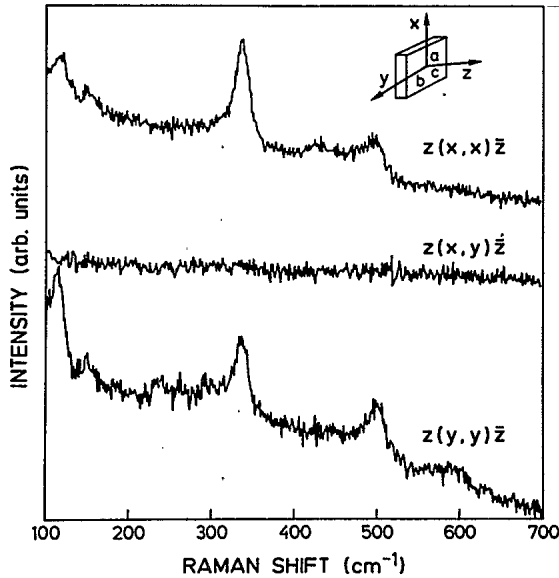


FIG. 2. Polarization-dependent Raman scattering spectra of a single crystal of  $\text{YBa}_2\text{Cu}_3\text{O}_{7-\delta}$ .

this crystal excited with an  $\text{Ar}^+$  laser (514.5 nm, 10 mW).  $x$  and  $y$  refer to polarization  $\hat{e}_i$  and  $\hat{e}_s$  of the incident and scattered electric fields along the  $a$  and  $b$  axes of the crystal. In Fig. 2, we present only the case of light propagation vectors parallel to the  $c$  axis; for a complete analysis of the selection rules with other polarizations, see Ref. 6 (when rotating the samples  $45^\circ$  around  $z$  the polarized-depolarized behavior of the  $335\text{-cm}^{-1}$  peak reverses while all others remain the same). The upper curve shows clearly the five Raman-active  $A_g$  modes at 120, 154, 335, 435, and  $500\text{ cm}^{-1}$ . Also shown is the response under crossed polarizations where, due to the diagonal Raman tensors, no scattering is allowed. In the lower curve we see the response of the single crystal for  $\hat{e}_i \parallel \hat{e}_s \parallel \hat{b}$ . It also contains all Raman allowed peaks. They have, however, different intensities than in the upper curve. While the amplitude of the peak at  $335\text{ cm}^{-1}$  is decreased by a factor of 0.7, the peaks at 120 and  $500\text{ cm}^{-1}$  become stronger by a factor of 3–4 and 1.8, respectively. The peak at  $154\text{ cm}^{-1}$  remains approximately constant. These differences are entirely consistent with the orthorhombic symmetry of the crystal if one assumes that the dominant contribution to the Raman polarizability comes from the Cu–O and O–O interactions.

The calculated eigenvectors of the mode at  $335\text{ cm}^{-1}$ , for example, consist of motions of the O(2) and O(3) atoms in  $\pm z$  direction. In the tetragonal crystal, the magnitudes of O(2) and O(3) displacements are equal,<sup>16</sup> but they change somewhat when the additional oxygen atom introduces orthorhombic symmetry.<sup>6</sup> A quantitative estimate of this change depends on the details of the lattice dynamical calculation, but it can be said generally that the repulsive interaction of the O(1) and O(3) ( $b$ -axis) atoms reduces the displacement of the latter. There is hence a larger bond polarizability for polarizations along the  $a$  axis as evidenced by the larger amplitude of the peak at  $335\text{ cm}^{-1}$  in the corresponding curve.

The main contribution to the in-plane polarizability of the Cu(1)–O(4) vibration at  $500\text{ cm}^{-1}$  should come from the Cu(1)–O(1) bond. Thus the scattering efficiency should be larger when the electric fields are oriented along the in-plane component of the O–O interaction, i.e., the  $b$  axis. Similarly, one finds that the additional Ba–O bond for  $\delta=0$  partially cancels the polarizability of the Ba–O(3) bond and enhances the peak when  $\hat{e}_i \parallel \hat{e}_s \parallel \hat{b}$ . The enhancement of both peaks is seen in Fig. 1.

The Cu(2) vibration ( $154\text{ cm}^{-1}$ ), on the other hand, does not appear to change amplitude for excitation along the two different crystal axes. This is reasonable since the atom O(1) causing orthorhombicity is far from the copper atom which then feels no additional anisotropic polarizability. The difference in lattice constants alone is too small to produce a measurable effect on the phonon peak amplitude. The in-phase  $435\text{ cm}^{-1}$  oxygen frame vibration is too weak in Fig. 2 to make reliable statements on its amplitude; it is, however, expected that it shows the opposite behavior to the  $335\text{-cm}^{-1}$  mode due to the reversal of the magnitudes of the O(2) and O(3) eigenvectors.

In searching for the element that most strongly feels the broken tetragonal symmetry, one is led to vibrations of the O(1) atoms which are, however, Raman forbidden. The modes where O(1) is out of phase with Cu(1) have been calculated to be at  $\sim 576$  and  $130\text{ cm}^{-1}$  for  $y$  and  $x$  directions, respectively.<sup>6</sup> The corresponding in-phase modes are at  $156$  and  $62\text{ cm}^{-1}$ . The vibration at  $576\text{ cm}^{-1}$  has been clearly identified in the far-infrared spectra.<sup>2,6</sup> It has been suggested that peaks corresponding to these vibrations are seen—defect induced—in the Raman spectra of crystals as well.<sup>6</sup> In Fig. 2, two weak peaks, at  $580$  and  $220\text{ cm}^{-1}$ , show strong orthorhombic character. They appear for  $\hat{e}_i \parallel \hat{e}_s \parallel \hat{b}$  while they are absent for  $\hat{e}_i \parallel \hat{e}_s \parallel \hat{a}$ . This implies a strong Raman polarizability in the direction of the chains;  $\alpha_{yy}$  is the only nonzero Raman tensor element ( $\alpha_{zz} \approx 0$  for these two modes was concluded in Ref. 6). For the high-energy peak, a large longitudinal polarizability of each O(1)–Cu(1) bond can be expected but it must vanish when adding up all bonds of an infinite chain. Oxygen deficiency should make the mode Raman allowed. From the complete set of eigenvectors of  $\text{YBa}_2\text{Cu}_3\text{O}_{7-\delta}$ , only the in-phase and out-of-phase O(1)–Cu(1) vibrations fulfill these requirements. The  $220\text{-cm}^{-1}$  mode obtains its Raman polarizability from a difference of factor 1.5 in displacements of the O(1) and Cu(1) atoms.<sup>6</sup> The two modes are expected to have a strong dependence on oxygen content. This has been confirmed in a systematic study for different  $\delta$ . The peaks at  $220$  and  $580\text{ cm}^{-1}$  are very weak for  $\delta \approx 0$  and 1: for  $\delta \rightarrow 0$  the active bond is reduced in concentration and for  $\delta \rightarrow 1$ , the chains become more perfect, and hence, more Raman forbidden.<sup>17</sup> From the Raman results above it can be concluded that our specimen has orthorhombic character. Together with the x-ray analysis, this constitutes an unprecedented report of the  $a$ - $b$  anisotropy in high- $T_c$  superconducting crystals.

We further chose to investigate the anomalous temperature dependence of the  $335\text{-cm}^{-1}$  Raman phonon in our high-quality untwinned crystal. After the initial report of Ref. 10, it has been confirmed to occur in many superconducting samples.<sup>11,18</sup> Furthermore, it was reported in the

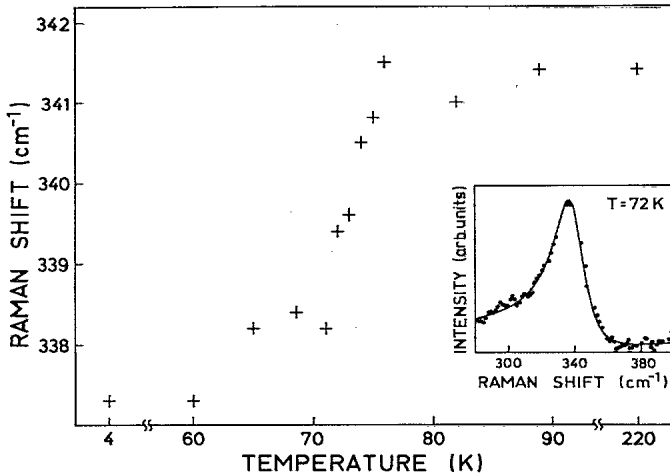


FIG. 3. Anomalous softening of the  $335\text{-cm}^{-1}$  phonon when  $\text{YBa}_2\text{Cu}_3\text{O}_{7-\delta}$  is cooled below  $T_c$ . The inset shows the fit of a Fano function to the phonon peak at  $T=72\text{ K}$  (see text).

far-infrared (FIR) measurements for the phonons at  $275$  and  $310\text{ cm}^{-1}$ .<sup>18</sup> The magnitude of the observed shifts in the FIR is about  $10\text{ cm}^{-1}$  while it amounts to  $\sim 5\text{ cm}^{-1}$  in Raman scattering. The Raman anomaly is absent<sup>16</sup> for samples with low-oxygen content ( $\delta \approx 1$ ). It has hence been speculated that the phonon softening is related to the opening of a superconducting gap close to but above the phonon frequency. We have measured the frequency of the  $335\text{-cm}^{-1}$  phonon near  $T_c$ . In Fig. 3 we show that the peak frequency  $\omega_0$  shifts predominantly within an interval of  $10\text{ K}$ . The frequencies were determined by fitting the phonon peak to Fano line shapes which should represent the interaction of the phonon with the electronic continuum.<sup>19</sup>

$$f(\epsilon) = \frac{(q + \epsilon)^2}{1 + \epsilon^2}, \quad (1)$$

where  $\epsilon = (\omega - \omega_0)/\Gamma$  is the reduced frequency. The parameter  $q$  accounts for the asymmetry of the observed line shape. It is worth mentioning that in the nonsuperconducting material no significant asymmetry is observed. While relative temperatures were known to better than  $0.2\text{ K}$ , the absolute temperatures were affected by an imperfect thermal contact of the crystal with the cold finger. We estimate the temperature increase by observing the frequency shift at a laser power reduced from  $10\text{ mW}$  to  $5\text{ mW}$  and find that the actual temperature in Fig. 3 is  $\sim 10 \pm 5\text{ K}$  above the nominal one. The frequency shift hence occurs approximately at  $T_c$ . This observation reveals that a gap opens in the sample when it undergoes the transition to the superconducting state. This gap must be positioned near the phonon ( $335\text{ cm}^{-1}$ ) and above it.<sup>20,21</sup>

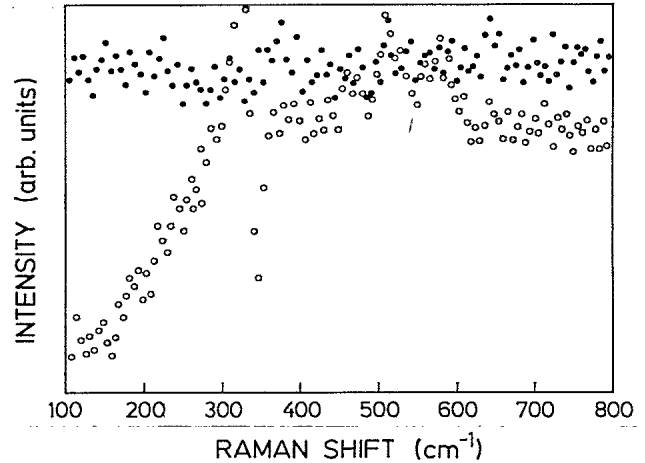


FIG. 4. Background scattering of a single crystal for two temperatures. The curves were obtained by subtracting the spectrum at  $T=100\text{ K}$  from the spectrum at  $4\text{ K}$  (open circles) and at  $89\text{ K}$  (solid circles).

An analysis of this phonon shift (self-energy) based on the nearly tetragonal nature of the  $335\text{-cm}^{-1}$  mode has been made by Zeyher and Zwicky.<sup>21</sup>

Other attempts to detect the superconducting gap by Raman scattering have been presented.<sup>22</sup> Here the change in scattering over a broad range of frequencies was observed when the sample was cooled below  $T_c$ . In the untwinned single crystal investigated here, we find a reduced background scattering below  $T_c$  at frequency  $\leq 300\text{ cm}^{-1}$  confirming those observations (Fig. 4).

In conclusion, we have presented optical measurements which demonstrate the orthorhombic symmetry of an untwinned single crystal of  $\text{YBa}_2\text{Cu}_3\text{O}_{7-\delta}$ . Strong evidence was found for a connection between the phonon anomaly and a superconducting gap. Theories involving grain boundaries as a necessary component of the high- $T_c$  phenomenon can be discarded in view of the evidence presented here.

*Note added in proof.* S. L. Cooper, M. V. Klein, B. G. Pazol, J. P. Rice, and D. M. Ginsberg [Phys. Rev. B **37**, 5920 (1988)] have reported data similar to those presented here. They interpret the fact that the intensity of Fig. 4 below  $T_c$  does not become zero at any frequency as meaning that there are excitations with zero gap in the superconductor.

We would like to thank R. Kremer for the magnetic measurements, L. Walz for the crystallographic data, and E. Schönherr for valuable discussions. H. Hirt, M. Siemers, and P. Wurster have given us expert technical help.

<sup>1</sup>M. Stavola, D. M. Krol, W. Weber, S. A. Sunshine, A. Jayaraman, G. A. Kourouklis, R. J. Cava, and E. A. Rietman, Phys. Rev. B **36**, 850 (1987).

<sup>2</sup>M. Cardona, L. Genzel, R. Liu, A. Wittlin, H. J. Mattausch, F. García-Alvarado, and J. M. García-Gonzalez, Solid State

Commun. **64**, 727 (1987).

<sup>3</sup>H. Rosen, E. M. Engler, T. C. Strand, V. Y. Lea, and D. Bethme, Phys. Rev. B **36**, 726 (1987).

<sup>4</sup>D. A. Bonn, J. E. Greendau, C. V. Stager, T. Timusk, M. G. Doss, S. L. Herr, K. Kamarás, and D. B. Tanner, Phys. Rev.

- Lett. **58**, 2249 (1987).
- <sup>5</sup>Y. Morioka, M. Kikuchi, and Y. Syono, *Jpn. J. Appl. Phys.* **26**, L1499 (1987).
- <sup>6</sup>R. Liu, C. Thomsen, W. Kress, M. Cardona, B. Gegenheimer, F. W. de Wette, J. Prade, A. D. Kulkarni, and U. Schröder, *Phys. Rev. B* **37**, 7971 (1988).
- <sup>7</sup>R. Bhadra, T. O. Brun, M. A. Beno, B. Daborowski, D. G. Hinks, J. Z. Liu, J. D. Jorgensen, L. J. Novicki, A. P. Paulikas, Ivan K. Schuller, C. U. Segre, L. Soderholm, B. Veal, H. H. Wang, J. M. Williams, K. Zhang, and M. Grimsditch, *Phys. Rev. B* **37**, 5142 (1988).
- <sup>8</sup>D. M. Krol, M. Stavola, W. Weber, L. F. Schneemeyer, J. V. Waszczak, S. M. Zahurak, and S. G. Konsinski, *Phys. Rev. B* **36**, 8325 (1987); *Z. Schlesinger, R. T. Collins, D. L. Kaiser, and F. Holtzberg, Phys. Rev. Lett.* **59**, 1958 (1987).
- <sup>9</sup>A. Yamanaka, F. Minami, K. Watanabe, K. Inoue, S. Takekawa, and N. Iyi, *Jpn. J. Appl. Phys.* **26**, L1404 (1987).
- <sup>10</sup>R. M. Macfarlane, H. Rosen, and H. Seki, *Solid State Commun.* **63**, 831 (1987).
- <sup>11</sup>A. Wittlin, R. Liu, M. Cardona, L. Genzel, W. König, W. Bauhofer, H. J. Mattausch, A. Simon, and F. García-Alvarado, *Solid State Commun.* **64**, 477 (1987).
- <sup>12</sup>L. F. Schneemeyer, J. V. Waszczak, T. Siegrist, R. B. van Dover, L. W. Rupp, B. Batlogg, R. J. Cava, and D. V. Murphy, *Nature* **328**, 601 (1987).
- <sup>13</sup>T. Siegrist, L. F. Schneemeyer, J. Waszczak, N. P. Singh, R. L. Opila, B. Batlogg, L. W. Rupp, and D. V. Murphy, *Phys. Rev. B* **36**, 8365 (1987).
- <sup>14</sup>J. L. Hodeau, C. Chaillout, J. J. Capponi, and M. Marezio, *Solid State Commun.* **64**, 1349 (1987).
- <sup>15</sup>G. Roth, D. Ewert, G. Heger, M. Hervieu, C. Michel, B. Raveau, F. D'Yvoire, and A. Revcolevschi, *Z. Phys. B* **69**, 21 (1987).
- <sup>16</sup>C. Thomsen, M. Cardona, W. Kress, R. Liu, L. Genzel, M. Bauer, E. Schönherr, and U. Schröder, *Solid State Commun.* **65**, 1139 (1988).
- <sup>17</sup>C. Thomsen, R. Liu, M. Bauer, A. Wittlin, L. Genzel, M. Cardona, E. Schönherr, W. Bauhofer, and W. König, *Solid State Commun.* **65**, 55 (1988).
- <sup>18</sup>M. Cardona, R. Liu, C. Thomsen, M. Bauer, L. Genzel, W. König, A. Wittlin, U. Amador, M. Barahona, F. Fernández, C. Otero, and R. Sáez, *Solid State Commun.* **65**, 71 (1988).
- <sup>19</sup>U. Fano, *Phys. Rev.* **124**, 1866 (1961).
- <sup>20</sup>P. B. Littlewood and C. M. Varma, *Phys. Rev. Lett.* **47**, 811 (1981).
- <sup>21</sup>R. Zeyher and G. Zwicknagl (unpublished).
- <sup>22</sup>K. B. Lyons, S. H. Lion, M. Hong, H. S. Chen, J. Kwo, and T. J. Negran, *Phys. Rev. B* **36**, 5592 (1987).
- <sup>23</sup>A. V. Bazhenov, A. V. Gorbunov, N. V. Klassen, S. F. Kodakov, I. V. Kukushkin, V. D. Kalakovskii, O. V. Misochko, V. B. Timofeev, L. I. Chernyshova, and B. N. Shepel, *Novel Superconductivity*, edited by S. A. Wolf and V. Z. Kresin (Plenum, New York, 1987), p. 893.